

Spiral waves in accretion discs – theory

Henri M. J. Bön

Royal Observatory of Belgium, Avenue Circulaire 3, B-1180 Brussels
Henri.Bon@oma.be

Abstract. Spiral shocks have been widely studied in the context of galactic dynamics and protostellar discs. They may however also play an important role in some classes of close binary stars, and more particularly in cataclysmic variables. In this paper, we review the physics of spiral waves in accretion discs, present the results of numerical simulations and consider whether theory can be reconciled with observations.

If, in the course of the evolution of a binary system, the separation between the stars decreases, there comes a point where the gravitational pull of one of the stars becomes matter from its companion. There is mass transfer, through the so-called Roche lobe overflow. This is what is believed to happen in cataclysmic variable stars (CVs; see Warner [40] for a review). In these, a white dwarf primary removes mass from its low-mass late-type companion which fills its Roche lobe. In this particular case, the decrease in the separation is due to a loss of angular momentum by magnetic braking or by gravitational radiation.

1 Roche lobe

Consider a binary system with a primary white dwarf of mass M_1 , and a companion of mass M_2 with a mean separation a . We can define the mass ratio, $q = M_1/M_2$, which, for CVs, is generally smaller than 1. From Kepler's law, the orbital period, P_{orb} , is then:

$$P_{orb}^2 = \frac{4\pi^2 a^3}{G(M_1 + M_2)}; \quad (1)$$

G being the gravitational constant, and the masses being expressed in units of the solar mass.

In the reference frame rotating with the binary and with the center of mass at the origin, the gas flow is governed by Euler's equation:

$$\frac{\partial \mathbf{v}}{\partial t} + (\mathbf{v} \cdot \nabla) \mathbf{v} = -\nabla \Phi - \frac{1}{r} \frac{\partial}{\partial r} (r^2 \Omega^2 \mathbf{r}); \quad (2)$$

where Ω is the angular velocity of the binary system relative to an inertial frame, and is normal to the orbital plane with a module $\Omega = 2\pi/P$; \mathbf{r} is the

density and P is the pressure. The last term in the right hand side of this equation is thus the gas pressure gradient, while the second is the Coriolis force. Here, Φ_r is the Roche potential, and includes the effect of both gravitational and centrifugal forces :

$$\Phi_r = -\frac{GM_1}{|\mathbf{r} - \mathbf{r}_1|} - \frac{GM_2}{|\mathbf{r} - \mathbf{r}_2|} - \frac{1}{2}(\Omega - \dot{\phi})^2 r^2; \quad (3)$$

where $\mathbf{r}_1, \mathbf{r}_2$ are the position vectors of the centres of the two stars. The equipotential surfaces of Φ_r are shown in Fig. 1. It can be seen that there is a particular equipotential which delimits the two Roche lobes of the stars. The saddle point where the two lobes join is called the inner Lagrange point, L_1 . These Roche lobes are the key to understanding mass transfer in close binary systems. Indeed, if one of the two stars fills its Roche lobe, then matter can move into the Roche lobe of its companion and be gravitationally captured by it. Mass transfer occurs via the so-called Roche lobe overflow mechanism. The size of the Roche lobes, R_{L1} and R_{L2} , in unit of the separation is only a function of the mass ratio, $R_{L2} = a f(q)$ and $R_{L1} = a f(q^{-1})$, where an approximate value for $f(q)$ is given by

$$f(q) = \begin{cases} 0.38 + 0.20 \log q & (0.3 < q < 20); \\ 0.462 \frac{q}{1+q} & (0 < q < 0.3); \end{cases} \quad (4)$$

From Eq.(1) and (4), one can see that the mean density of a star which fills its Roche lobe is a function of the orbital period only [40]:

$$\rho = \frac{107}{P_{\text{orb}}^2} \text{ g cm}^{-3}; \quad (5)$$

if P_{orb} is expressed in hours. Thus, for the typical orbital periods of CVs, from 1 to 10 hours, the mean density obtained is typical of lower main-sequence stars.

2 Disc formation

Matter which is transferred through the L_1 point to the companion has a rather high specific angular momentum with respect to the later, b_1^2 ! . Here, b_1 is the distance of the inner Lagrangian point to the centre of the primary and can be obtained with the following fitted formula :

$$b_1 = (0.500 - 0.227 \log q) a; \quad (6)$$

Once the gas comes close to the primary, it will mainly feel its gravitational force and follow a Keplerian orbit, for which the circular velocity is given by

$$v_c(r) = \sqrt{\frac{GM_1}{r}}; \quad (7)$$

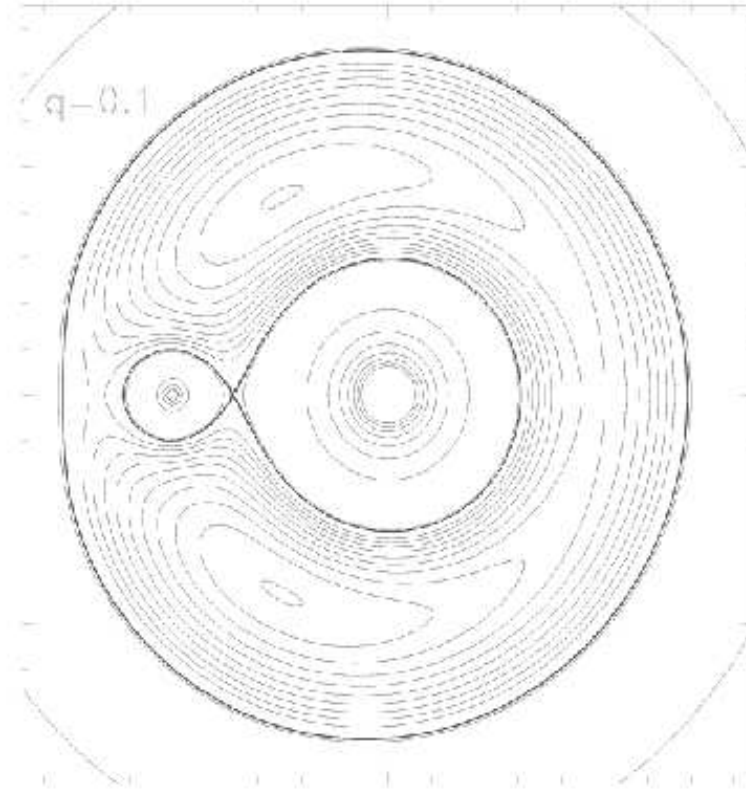


Fig. 1. Roche equipotentials in a binary system with a mass ratio, $q = 0.1$. The Roche lobes are shown with the heavy lines. The primary is in the middle

and the associated angular momentum, $r v_\phi(r)$. If we equal this to the angular momentum of the gas transferred through the Roche lobe, we can define the circularization radius $R_{\text{circ}} = (1 + q) (b_1/a)^4 a$. Gas coming from the companion will thus form a ring of radius approximately R_{circ} , provided this is larger than the radius of the accreting object. For cataclysmic variable stars, we typically have $P_{\text{orb}} = 1 - 10$ hours, $M_1 \approx M$ and $q < 1$. Therefore, $a \approx 3R$ and $R_{\text{circ}} \approx 0.1 - 0.3 a$. By comparison, the primary white dwarf has a radius about $0.01 R$. Thus, in non-magnetic CVs, the mass transfer will always lead to the formation of such a ring. This ring will then spread out by viscous processes: because energy is lost, the gas will move deeper into the gravitational well until it reaches the primary and accretion will occur (see [6]). To conserve angular momentum, the outer part will have to move further away. An accretion disc forms. The formation of an accretion disc is pictured in Fig. 2 as obtained from numerical simulations.

In principle, the disc could expand forever. In a binary system, this is not possible however because of the torque exerted by the companion. The radius

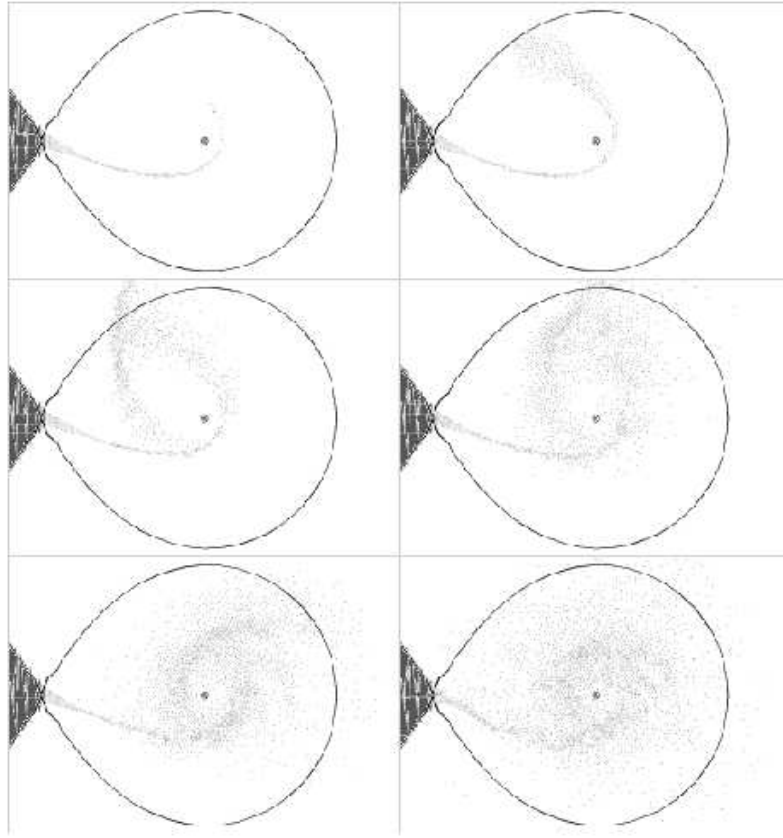


Fig.2. The formation of an accretion disc by Roche lobe overflow. The low mass transferring secondary is at the left. Mass flows through the inner Lagrange L_1 point towards the white dwarf primary

of the disc is therefore limited by the tidal radius, where the tides induced by the secondary star truncate the disc. The angular momentum is then transferred back to the orbital motion. Paczynski [24] has computed the maximum size of a disc in a binary system by following the orbits of a set of particles and deriving the largest non-intersecting orbit. This orbit would represent the maximum size of an accretion disc, when neglecting the effect of viscosity and pressure. This is called the disc's tidal truncation radius. Typically, the disc radius is limited to 0.7-0.9 the Roche lobe radius.

3 Viscosity

As we have seen, viscous processes are at play to explain the formation of accretion discs. It is this viscosity which will also ensure that matter transferred by the companion can be accreted onto the primary. In the thin disc approximation,

ie. when the disc half thickness H is much smaller than the radius r at each radius, $H/r \ll 1$, and in a steady state,

$$\nu = \frac{\dot{M}}{3} \frac{1}{\Sigma} \frac{R_{\text{wd}}}{r} \quad (8)$$

where ν is the effective kinematic viscosity, Σ the surface density and \dot{M} the mass accretion rate (e.g. [6]). The origin of this viscosity is as yet unknown. Shakura & Sunyaev [32] used a parametric formulation to hide in a parameter, α , our lack of knowledge:

$$\nu = \alpha c_s H \quad (9)$$

with c_s being the sound speed. Note that in the thin disc approximation,

$$\frac{H}{r} = \frac{c_s}{v} \frac{1}{M} \quad (10)$$

with M the Mach number in the disc. In the framework of the turbulent viscosity mechanism, the Shakura & Sunyaev prescription can be understood in writing the kinematic viscosity as the product of the turbulent velocity, v_t and the typical eddy size, l_{ed} : $\nu = v_t l_{\text{ed}}$. The eddy size cannot be larger than the disc scale height, thus $l_{\text{ed}} \leq H$. Moreover, in order to avoid shocks, the turbulent velocity must be subsonic, $v_t \leq c_s$. Thus, ν must be smaller or equal to 1. There is no reason however for ν to be constant throughout the disc.

By using Eq. (8) and the direct relation between the mass accretion rate and the luminosity of the disc, it is possible to have an estimate of the amount of viscosity present in the accretion disc of cataclysmic variables. In a typical dwarf nova, the disc is observed to brighten by about five magnitudes for a period of days every few months or so. According to the thermal instability model, which is the most widely accepted model to explain these outbursts, the disc slips from a low accretion, cool state in quiescence to a high accretion hot state at outburst (e.g. [39]). It is therefore generally believed that $\alpha \sim 0.01$ in quiescent dwarf nova, while α is typically 0.1-0.3 in dwarf novae in outburst or in nova-like stars. This is clearly too large by several order of magnitudes for standard molecular viscosity. More serious candidates are therefore turbulent viscosity, magnetic stresses and the Balbus-Hawley and Parker magnetic instabilities.

Although the common mechanisms invoked for this anomalous viscosity are thought to be local, hence the Shakura & Sunyaev prescription, it may be possible that some global mechanism is acting as a sink for angular momentum. In this case, one could still use the above prescription if we now use an effective parameter. This will be the case for spiral shocks which we will discuss in the rest of this review.

4 Spiral shocks

Although it was already known that accretion discs in close binary systems can lose angular momentum to an orbiting exterior companion through tidal

interaction [12,25], it is Sawada, Matsuda & Hachisu [29,30] who showed, in their 2D inviscid numerical simulations of accretion discs in a binary of unit mass ratio, that spiral shocks could form which propagate to very small radii. Spruit [34,35] and later Larson [11] made semi-analytical calculations which were followed by numerous mostly 2D numerical simulations [3,7,9,14,15,18,21,26,27,31,37,45]. An historic overview can be found in Matsuda et al. [22].

Savonije, Papaloizou & Lin [28] presented both linear and non-linear calculations of the tidal interaction of an accretion disc in close binary systems. The linear theory normally predicts that spiral waves are generated at Lindblad resonances in the disc. A main Lindblad resonance corresponds to the case where n times the disc angular speed is commensurate to m orbital angular speed:

$n = m!$, i.e. $r = \frac{1}{1+q} \left(\frac{n}{m}\right)^{2/3} a$. In fact, in their study of tidal torques on accretion discs in binary systems with extreme mass ratios, Lin & Papaloizou [13] already observed the spiral pattern. In their case, this pattern was indeed due to the 2:1 Lindblad resonance which can fall inside the Roche lobe and inside the disc if the mass ratio is small enough. However, the typical mass ratios and disc radius of cataclysmic variable stars does not allow the centre of such resonances to be in the disc. For the 2:1 resonance to lay inside the disc requires $q < 0.025$, a value too small for most cataclysmic variables although possible for some low-mass X-ray binaries. The 3:1 resonance can be located inside the disc for $q < 0.33$, hence for most of SU UMa stars (see e.g. [43]).

In their study, however, Lin & Papaloizou [13] showed that the resonant effect is significant over a region

$$x = \frac{r}{v} \frac{r_s^{1/3}}{r_s^2} r; \quad (11)$$

where r_s is the position of the resonance. Using $\Omega = c_s H$, this leads to $x / c_s^{2/3}$. Thus, as also found by Savonije et al. [28], even in CVs with larger mass ratios, the centre of the 2:1 resonance can still be thought of as lying in the vicinity of the boundaries of the disc and because the resonance has a finite width that increases with the magnitude of the sound speed, it can still generate a substantial wave-like spiral response in the disc, but only if the disc is large, inviscid and the Mach number is smaller than about 10. For larger Mach number, more typical of cataclysmic variables, however, Savonije et al. consider that wave excitation and propagation becomes ineffective and unable to reach small radii at significant amplitude.

We will look more closely to this later on. As for now, we will follow Spruit [34] to show why spiral waves can be thought of as an effective viscosity. Spiral waves in discs have been studied extensively in the context of galactic dynamics and of protostellar discs. Such waves carry a negative angular momentum. Their dissipation leads to accretion of the fluid supporting the waves onto the central object.

Consider some disturbance at the outer disc edge. As the generated wave propagates inward, it is being wound up by the differential Keplerian rotation

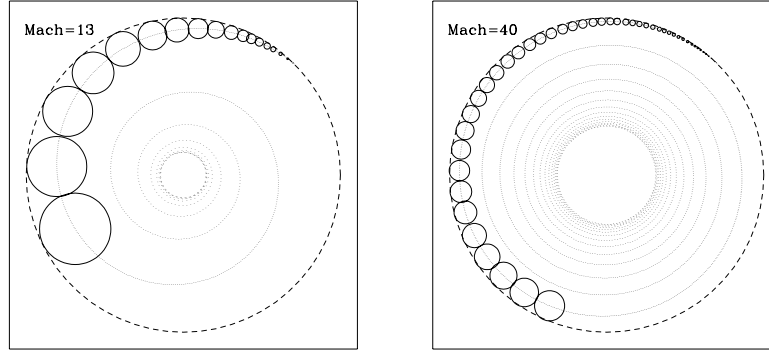


Fig. 3. Illustration of the fact that the angle of the spiral pattern depends on the Mach number. In the hot disc (left), the perturbation propagates faster and the spiral is more open than in the cold disc (right).

in the disc into a trailing spiral pattern (Fig. 3). The wave frequency for an azimuthal wavenumber m in the comoving frame is $\omega = \Omega - m\Omega'$, because we can neglect the much lower orbital frequency, Ω . The conserved wave action is given by

$$S_w = \frac{1}{2} \int^Z \frac{v_w^2}{v} dV \quad (12)$$

where v_w is the amplitude of the wave and the integration is carried out over the volume of the wave packet. The angular momentum of the wave, given by $j = m S_w$, is conserved, giving:

$$j = \frac{1}{2} \int^Z \frac{v_w^2}{v} dV \quad (13)$$

Hence, it is negative. This can be understood because the tidally excited spiral pattern rotates with the binary angular speed which is smaller than the angular speed of the gas in the disc.

Because of the differential rotation, the amplitude of the wave increases as it propagates inwards. Indeed, the radial extent of the wave packet, R , is proportional to the sound speed, $R \propto c_s$, while the volume of the wave packet is $V = 2H \pi R^2$. Now, because j is conserved, Spruit obtains

$$v_w \propto \frac{1}{r H c_s} \propto r^{-11/16}; \quad (14)$$

where in the last approximation, we made use of the relations valid for a thin disc. The wave therefore steepens into a shock. Dissipation in the shock leads to a loss of angular momentum in the disc, hence to accretion.

The opening angle of the spirals is related directly to the temperature of the disc as, when the shock is only of moderate strength, it roughly propagates at

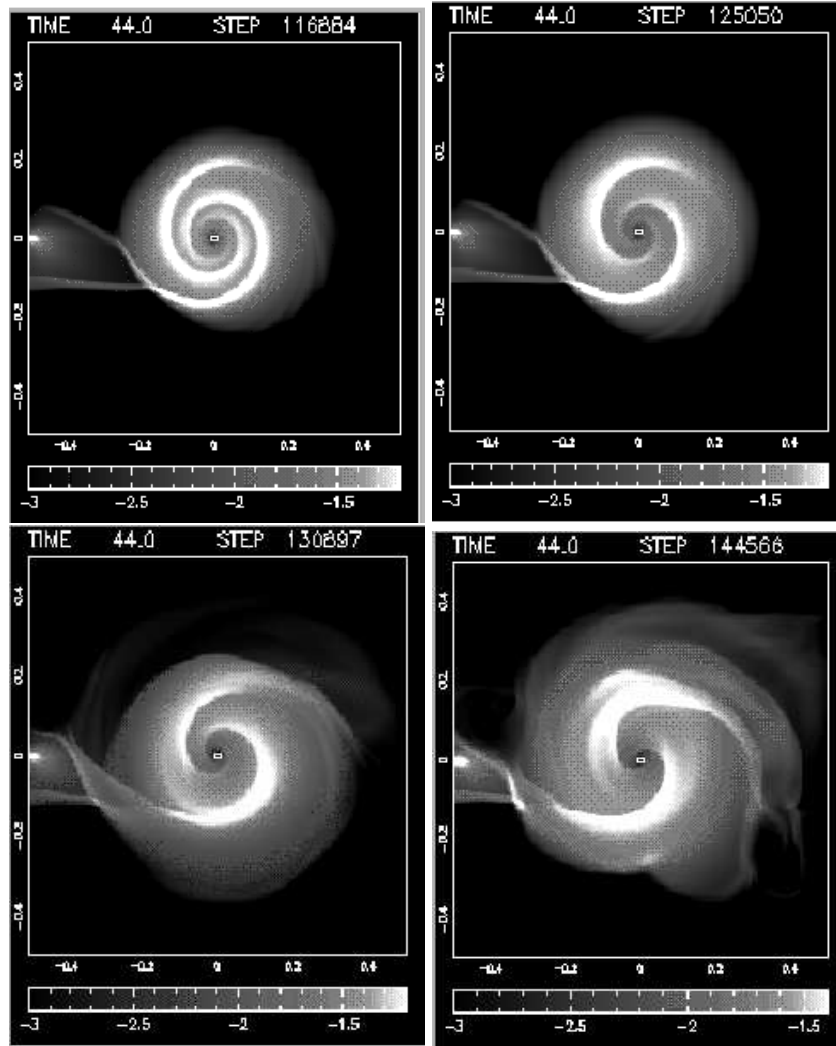


Fig. 4. Density plots of 2D finite-difference simulations (in the case of a mass ratio of 1) for different value of $\mu = 1.01$ (upper left), 1.05, 1.1, 1.2 (lower right). The scale is logarithmic and the results are shown at about 7 orbital periods [16]

sound speed. This is shown schematically in Fig. 3 for two values of the Mach number, where we have assumed that the perturbation propagates radially at a speed of 1.3 times the Mach number [2,10,34]. Thus the angle between the shock surface and the direction of the orbital motion is of the order $\tan^{-1} \frac{c_s}{v} = 1/M$. In the approximation of an adiabatic equation of state, often used in numerical simulations, where the temperature soon reaches a value given by $T = 0.5(\mu - 1)T_{\text{vir}}$, with T_{vir} being the virial temperature, the angle becomes

$P \approx 0.5 \left(\frac{M}{10^5} \right)^{-1/2}$. Thus, low mass discs will have more tightly wound spirals than large ones. This is indeed what is shown by two-dimensional simulations ([16,22]; see also Fig. 4).

5 Observational facts

The most prevalent and successful model to explain dwarf nova outbursts is the disc instability model based on a viscosity switch related to the ionisation of hydrogen in the disc. It is an hysteresis cycle, in which the disc switches back and forth between a hot optically thick high viscosity state – the outburst – and a cool optically thin low viscosity state – quiescence. The disc radius increases at outburst and then after maximum, decreases exponentially. In U Gem for example, a clear increase in the radius is seen at outburst: the radius of the disc is of the order of $0.4a$ at maximum and then it decreases on a timescale of tens of days to $0.28a$ [40]. While for EX Dra, Baptista & Catalan [1] found the disc radius to be $0.30a$ in quiescence and $0.49a$ in outburst.

Global disc evolution models reproduce the main properties of observed outbursts, but only if the efficiency of transport and dissipation is less in quiescence than during outburst [5]. This seems in agreement with spiral shocks. Indeed, the tidal force is a very steep function of $r=a$, hence the spirals rapidly become weak at smaller disc sizes. Spiral shocks are produced in the outer regions of the disc by the tides raised by the secondary star. During the outburst, the disc expands, and its outer parts feel the gravitational attraction of the secondary star more efficiently, leading to the formation of spiral arms.

Having these general ideas in mind, we can now summarise the results from observations (see the review by Danny Steeghs in this volume):

The spiral pattern has been established in several cataclysmic variables for a wide range of emission lines

The spiral arms appear right at the start of the outburst and persist during outburst maximum for at least 8 days, i.e. several tens of orbital periods

The structure is fixed in the corotating frame of the binary and corresponds to the location of tidally driven spiral waves

During quiescence, the spiral pattern is no longer there but the disc remains asymmetric

These results can be exactly interpreted in the spiral shock theory. They do not prove necessarily, however, that spiral shocks are the main viscosity mechanism in the disc. There is indeed a problem similar to the egg and the hen: who began? In order to have well developed spirals, one needs a large disc, which is due to an increase in viscosity!

6 Numerical simulations

As can already be seen from Fig. 3 and 4, in order to explain the widely open spirals seen in the Doppler maps of IP Peg [38], one requires a rather hot disc.

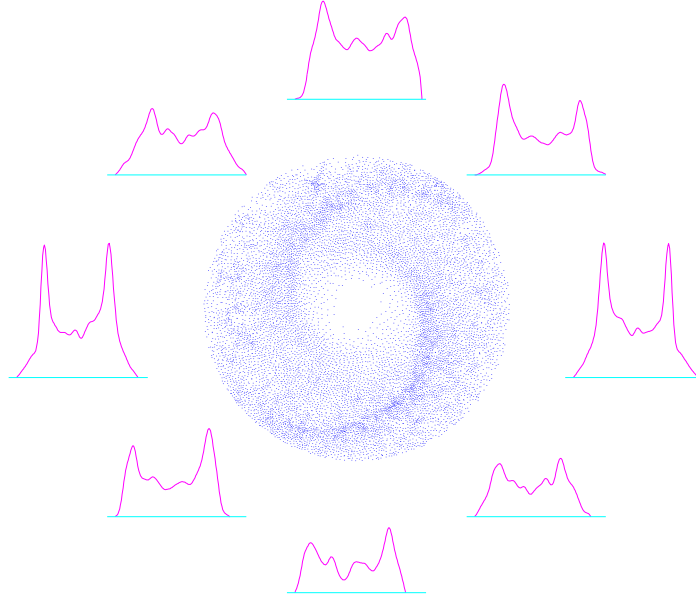


Fig. 5. An accretion disc showing spiral arms as obtained by SPH simulations. When viewed from different angles (i.e. at different orbital phases), the emission-line profile is different. When these lines are recorded at several orbital phases, one can then construct a spectrogram which can be inverted, using a maximum entropy method, to give a doppler tomogram

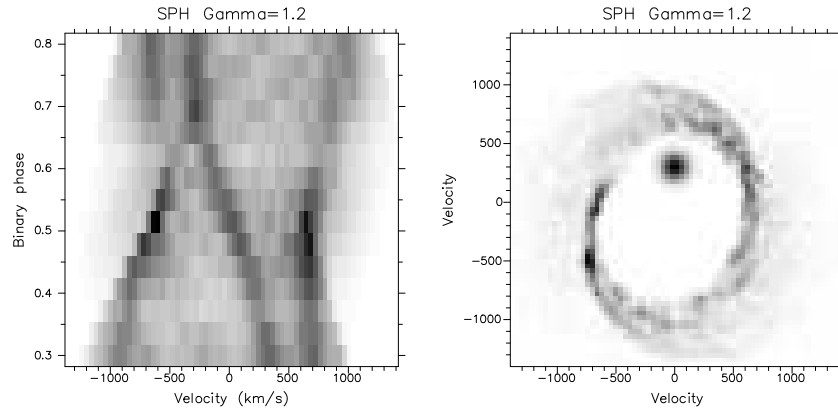


Fig. 6. Binary phase-velocity map (spectrogram) and Doppler map corresponding to the simulation of Fig. 5

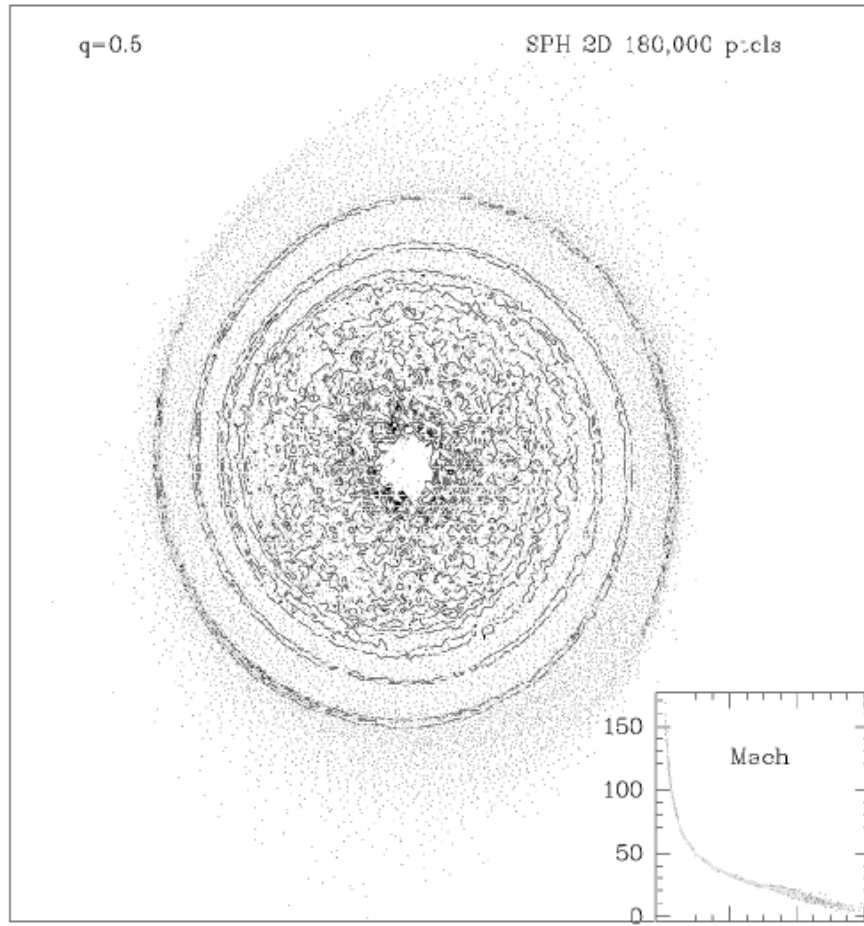


Fig. 7. Result of a high-resolution 2D SPH simulation of an isothermal ($c_s = 0.05$) accretion disc in a binary system with a mass ratio of 0.5. The density contours are plotted over the particles positions. The inset shows the variation of the Mach number with the distance from the white dwarf.

Figure 5 shows for example the results of a 2D numerical simulation, using the Smoothed Particle Hydrodynamics (SPH) method, of an accretion disc in a binary system with a mass ratio of 0.5, as observed for IP Peg. Here, a polytropic equation of state (EOS) has been used with a polytropic index, $n = 1.2$. In Fig. 5, we show the different emission lines profiles corresponding to the various orbital phases for such a disc. Those profiles can then be presented in a trailed spectrogram as seen in Fig. 6. With numerical simulations, we have the advantage of having all the dynamical information of the flow and we can therefore easily construct a Doppler map which can then be compared to those observed. The Doppler map corresponding to this $n = 1.2$, 2D simulation is also shown in Fig. 6. Note that we have artificially added a spot at the location of the sec-

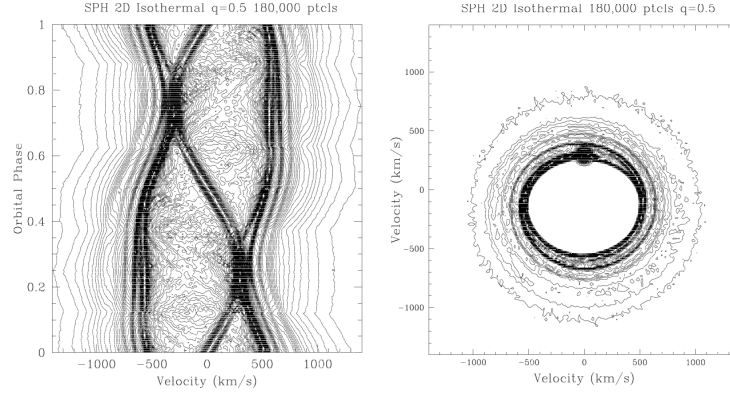


Fig. 8. Reconstructed trailed spectrogram and Doppler map from the numerical simulation shown in Fig. 7

ondary to allow more direct comparisons with real observations. It is obvious that even though this simulation was not the result of any tuning, the qualitative agreement between this calculated Doppler map and spectrogram, and the one first observed by Steeghs et al. [38] for IP Peg is very good. This however calls for some discussion. Indeed, in simulations using a polytropic EOS, as is the case here, the disc evolve towards the virial temperature and are therefore unphysically hot. There is thus an apparent contradiction between numerical simulations and observations. This was indeed the conclusions of the first few attempts to model the observed spirals in IP Peg in outburst. For comparison purposes, we present in Fig. 7 and 8, the results of a very high resolution isothermal simulation.

Godon, Livio & Lubow [8] presented two-dimensional disc simulations using Fourier-Chebyshev spectral methods and found that the spiral pattern resembles the observations only for very high temperatures. This was already the conclusion of Savonije et al. [28] who claimed that spirals could not appear in the colder disc of cataclysmic variables.

We have therefore run another set of simulations, with our SPH code, where we use an "isentropic" equation of state, instead of a polytropic one. By "isentropic", we mean a barotropic EOS, $P = K \rho^\gamma$, and keeping K constant. The heating due to the viscous processes is supposed to be instantaneously radiated away. In this case, the temperature remains always very close to the initial value. The results of isentropic runs are compared with those of polytropic runs using $\gamma = 1.2$ and two values for the initial sound speed: 0.1 and 0.04 times the orbital velocity (Fig. 9). While, in the two polytropic runs, spiral structures are clearly present with a very similar pitch angle, there is a clear distinction between the two isentropic runs: the 0.1 case produces well defined spiral arms which are more tightly wound than in the equivalent polytropic case, while in the 0.04 case, spiral structure can hardly be seen at all. The difference clearly lies in the Mach

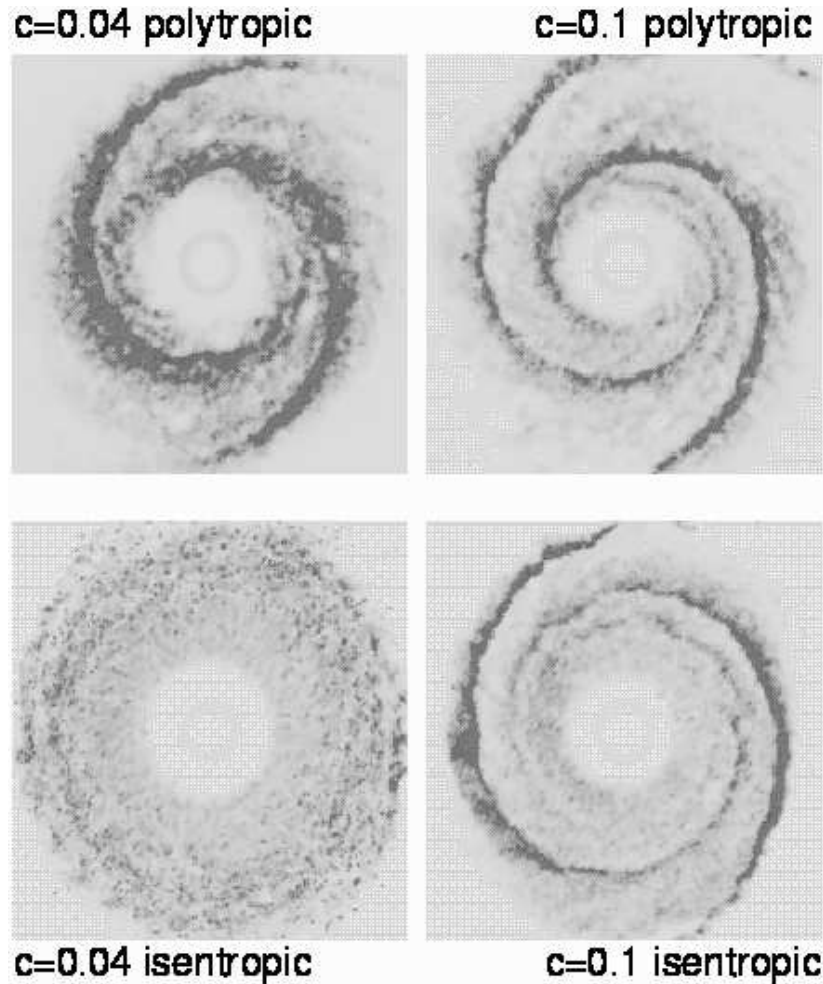


Fig. 9. Comparison between our SPH results for the isentropic and polytropic equation of state for two values of $c_s = 0.1$ and $c_s = 0.04$

number of the flow: in the polytropic cases, the Mach number is well below 10 for both a sound speed of 0.04 and 0.1, while in the isentropic cases, the Mach number goes from 20 at the outer edge of the disc to more than 100 inside when the sound speed is 0.04, but goes from 10 to only 30 when the sound speed is 0.1. Therefore, the observations seem to require a hot disc with a wide spiral. But, are dwarf novae discs hot or cold? During quiescence, the disc will have a temperature of the order of 10,000 K. This corresponds to a sound speed of the order of 15 km/s, or in our units 0.03. Thus, one should compare observations with our isentropic case with sound speed 0.04, and we therefore predict that no spiral should be seen. In outburst however, a dwarf nova will have a temperature profile corresponding to that of the steady-state solution for a viscous disc (e.g.

[40]), and the temperature will be closer to 10^5 K, i.e. a sound speed of roughly 45 km/s (in our units, 0.1). In this case, the Mach number will be around 20 and one is allowed to compare observations with the isentropic case with a sound speed of 0.1. Thus, one should clearly expect to see spiral structures in dwarf novae in outburst but not in quiescence.

Similarly, Stehle (1998) performed thin disc calculations where the full set of time dependent hydrodynamic equations is solved on a cylindrical grid. The disc thickness is explicitly followed by two additional equations in a one-zone model, allowing the disc to be vertically in non-equilibrium. The spatial and temporal evolution of the disc temperature follows tidal and viscous heating, the latter in the α -ansatz of Shakura & Sunayev, as well as radiation from the disc surfaces. The surface temperature is connected to the disc mid-plane temperature using Kramer's opacities for the vertical radiation transport. In this sense, it is a much more elaborated model than the classical isothermal or adiabatic approximation for the equation of state. Steeghs & Stehle (1999) use the grid of disc calculations of Stehle (1998) to construct Doppler tomograms for a binary with mass ratio $q = 0.3$ and orbital period $P = 2.3$ hours. They considered two models, one more typical of quiescent CVs, with $M' = 15-30$ and an α -type shear viscosity of 0.01, and another, representative of outbursting discs, with $M' = 5-20$ and $\alpha = 0.3$. Effective temperature ranged from less than 10^4 K in the outer part of the cold disc, to values between $2 \cdot 10^4$ and $5 \cdot 10^4$ K for the hotter disc. The cold disc was rather small (due to the low viscosity), varying in radius between 0.55 and 0.65 r_{L1} , while the hot disc is pushed by the increased viscosity to larger radii of 0.6-0.8 r_{L1} . For the high Mach number accretion discs, they find that the spiral shocks are so tightly wound that they leave few fingerprints in the emission lines, the double peaks separation varying by at most 8%. For the accretion disc in outburst, however, they conclude that the lines are dominated by the emission from an $m = 2$ spiral pattern in the disc, resulting in converging emission line peaks with a cross over near phases 0.25 and 0.75. It has to be noted that in the simulations of Stehle, it is the presence of a large initial shear viscosity (in the form of an α -type parameterization) which provides the viscous transport required to setup a large hot disc in which a strong two armed spiral pattern forms. This remark will take all its relevance in view of the discussion in Sect. 8.

For example, Godon et al. [8] used a value of $\alpha = 0.1$, so that viscous spreading was less efficient compared to the simulations of Stehle. As a consequence, their discs were smaller by up to 50% compared to the hot disc model of Steeghs & Stehle, hence the tidal effect was less severe.

7 Angular momentum transport

As noted above, the parameter α introduced by Shakura and Sunayev [32] refers to some local unknown viscosity. In the case of spiral shocks, which is a global phenomenon, we can still refer to an effective α that would give the same mass accretion rate in an α -disk model that one finds in numerical simulations.

The standard α -disc theory gives the mass accretion rate in terms of α as $\dot{M} = 3 \pi c_s H$ [see Eq. (8) and (9)]. Using Eq. (10), Blondin [2] finds an equation for α_e :

$$\alpha_e = \frac{2 v}{3} \frac{h v_r i}{c_s^2}; \quad (15)$$

where $h v_r i$ is a density-weighted average of the radial velocity:

$$h v_r i = \frac{\int_0^{R_2} v_r d}{\int_0^{R_2} d}.$$

It has to be noted that the accretion time scale can be estimated (e.g. [36]):

$$\frac{1}{\alpha_e} \frac{v}{c_s} :$$

Thus this time scale can only be followed for rather hot discs with high value of α_e and therefore, for cold discs, the evolution can usually be followed until the wave pattern is stationary but not long enough for the accretion process to reach a steady state. The wave pattern on the other hand is stable in only a few sound crossing time.

From his study of self-similar models of very cool discs, Spruit [34] obtains $\alpha_e = 0.013 \frac{H}{r}^{3/2}$. As in cataclysmic variables, $\frac{H}{r} \approx 0.1$, this leads to very low values (10^{-4} – 10^{-3}), which was the reason why several people dismissed spiral shocks as a viable efficient accretion mechanism. Spruit himself, however, in his paper, insists that this must not be the final word: "Formost common mass ratios $0.1 < q < 1$, the forcing by the companion is so strong however that the resulting spiral shock therefore have a strength much above the self-similar value over a large part of the disc". In their inviscid – but adiabatic – simulations, Matsuda et al. (1987) obtained values of the efficiency up to 0.1, hence large enough to explain mass accretion observed in outbursting cataclysmic variables. In fact, Spruit [34] and Larson [10] obtained a relation between the efficiency and the radial Mach number M_r at disc mid-plane. Larson [10], for example, obtains $\alpha_e \approx 0.07 (M_r^2 - 1)^3$ for isothermal discs. Note that for an isothermal disc, M_r^2 is equal to the compression ratio. With M_r being of the order of 1.3 to 1.5, this typically implies values of $\alpha_e \approx 0.02$ – 0.14 . Numerical simulations by Blondin [2] seem to confirm this, as in his isothermal simulations, values as high as 0.1 are obtained near the outer edge of the disc. For very cold discs, he even found values close to 1. The accretion efficiency however decreases very sharply and reaches value below 10^{-3} in the part of the disc closer than 0.1a. For a hotter disc, if the value of α_e is about 0.1 in the outer part of the disc, it stays above 0.01 well inside the disc. Larson [10] goes on to predict that the strength of tightly wound spiral shocks in a cold, thin disk should be proportional to $(\cos \theta)^{3/2}$, where θ is the trailing angle of the spiral wave. Estimating $\cos \theta \approx 1.5 c_s / v$, Larson [10] finds an efficiency of

$$0.026 \frac{c_s}{v}^{3/2} : \quad (16)$$

The prediction for an isothermal disk with $c_s = 0.25$ is $3.2 \times 10^{-3} r^{3/4}$, orders of magnitude below that found in the numerical simulations (e.g. [2,18]). But in these simulations, the spirals are not tightly wound and the formula of Larson may not be applicable.

Blondin [2], for example, finds that the maximum value of \dot{M} , found near the outer edge of the disk, remains roughly independent of sound speed, while the radial dependence of $\dot{M}(r)$ steepens with decreasing sound speed. In fact, because the radial decay of \dot{M} is so steep, he found steady mass accretion only for radii above $r \approx 0.1a$ in the coldest disk with an outer Mach number of ≈ 3.2 . A further result of his simulations is the relative independence of spiral waves on the mass ratio in the binary system. The strength of the two-armed spiral shocks at their origin near the outer edge of the disk was fairly constant in all of his models. Blondin believes this has the consequence that, despite all else, one can be confident that the effective \dot{M} in the outer regions of an accretion disk in a binary system is (at least) ≈ 0.1 .

8 Spirals in quiescence ?

By using results from shearing-box simulations as an input for a global numerical model designed to study disc instabilities, Menou [23] shows that as the disc goes into quiescence, it suffers a runaway cooling. Hence, in quiescence, the disappearance of self-sustained MHD turbulence is guaranteed. As accretion is known to occur during quiescence in cataclysmic variables, another transport mechanism must operate in the discs. The rapid disc expansion observed during the outbursts of several dwarf novae is consistent with MHD-driven accretion because it shows that disc internal stresses dominate transport during this phase [23]. On the other hand, the same discs are observed to shrink between consecutive outbursts, which is a signature that transport is dominated by the tidal torque due to the companion star, at least in the outer regions of the disc during quiescence. When looking at a sample of 6 well studied SU UMa stars, Menou [23] finds an anti-correlation of the recurrence times with mass ratios. This, he interprets, is evidence that tidal torques dominate the transport in the quiescent discs. Indeed, the recurrence times of dwarf novae represent the time-scales for mass and angular momentum redistribution in the quiescent discs. For his small sample, the correlation is significant for normal and super-outbursts. No correlation is however found for U Gem type dwarf novae but this could be because the correlation is masked by other effects. Menou [23] proposes thus the concept of accretion driven by MHD turbulence during outburst and by tidal perturbations during quiescence.

This is, at first sight, a rather astonishing result. Indeed, we have seen that the spirals will be more developed and more effective when the disc is hotter and larger, i.e. in outburst. If the main source of viscosity during quiescence are the spiral shocks, then one might expect that their contribution during outburst cannot be negligible. But as stated before, one needs first to make the disc large for the tidal effect to become more important. The answer may lie – like

always – in a combination of processes. Spiral arms are indeed very good at transporting angular momentum in the outer part of the disc. But they do not succeed generally to penetrate deep into the disc. This is where MHD turbulence may provide the main source of viscosity. This scenario clearly needs to be further developed and tested.

9 Spiral shocks in other stellar objects

Even if spiral shocks are not the main driving viscosity mechanism in accretion discs, Murray et al. (1998) argue that they could have another observational consequence in intermediate polars. Indeed, the presence of spiral waves break the axisymmetry of the inner disc and tells the accreting star the orbital phase of its companion. This could put an additional variation in the accretion rate onto the white dwarf, a variation dependent on the orbital period. This could explain the observed periodic emission in intermediate polars.

Savonije, Papaloizou & Lin [28] note that although tidally induced density waves may not be the dominant carrier of mass and angular momentum throughout discs in CVs, they are more likely to play an important role in protostellar discs around T Tauri binary stars, where the Mach number is relatively small. In GW Ori for example, both circumstellar and circumbinary discs have been inferred from infrared excesses [17] and the disc response to the tidal disturbance might be significant. In the same line of ideas, Bon et al. [4,41,42,44] found large tidal waves in large protostellar discs being induced by the tidal interaction of a passing star. In this case, the perturbation might be large enough in these self-gravitating discs to lead to the collapse of some of the gas, thereby forming new stars as well as brown dwarfs and jovian planets.

Another class of objects where spiral arms may play a role is X-ray binaries (see the review by E. Harlaftis in this volume). There also, because the discs are rather hot, the Mach number is much smaller than in CVs, hence their effect might be more pronounced. An observational confirmation of this would be most welcome. The work of Soria et al. [33] is maybe such a first step. These authors studied optical spectra of the soft X-ray transient GRO J1655-40. They claim that, during the high state, the Balmer emission appears to come only from a double-armed region on the disc, possibly the locations of tidal density waves or spiral shocks.

References

1. Baptista R., Catalan M. S., 2000, *ApJ*, 539, L55
2. Blondin, 1999, *New Astronomy*, 5, 53
3. Bon H M J, Haraguchi K., Matsuda T., 1999, In: *Disk Instabilities in Close Binary Systems | 25 Years of the Disk-Instability Model*, Mineshige S., Wheeler J.C., eds., Universal Academy Press, p. 137
4. Bon H M J., Watkins S.J., Bhattal A.S., Francis N., Whitworth A.P., *MNRAS*, 300, 1189

5. Cannizzo J.K., 1993, In: *Accretion disks in Compact Stellar Systems*, Wheeler J.C., ed., p. 6
6. Frank J., King A.R., Raine D.J., 1992, *Accretion Power in Astrophysics*, 2nd ed., Cambridge University Press
7. Godon P., 1997, *ApJ*, 480, 329
8. Godon P., Livio M., Lubow S., 1998, *MNRAS*, 295, L11
9. Haraguchi K., Bon H.M.J., Matsuda T., 1999, In: *Star Formation*, p. 241
10. Larson R.B. 1989, In: *The Formation and Evolution of Planetary Systems*, H.A. Weaver & L.D. Anly, eds., Cambridge Univ. Press, p. 31
11. Larson R.B., 1990, *MNRAS*, 243, 358
12. Lin D.N.C., Pingle J.E., 1976, In: *Structure and Evolution of Close Binary Systems*, Eggleton P., Mitton S., Whelan J., eds., *Proc. IAU Symp. 73*, Reidel, p. 237
13. Lin D.N.C., Papalbizou J., 1979, *MNRAS*, 186, 799
14. Makita M., Matsuda T., 1999, In: *Numerical Astrophysics*, Miyama S.M., Tomisaka K., Hanawa T., eds., Kluwer, p. 227
15. Makita M., Yukawa H., Matsuda T., Bon H.M.J., 1999, In: *Disk Instabilities in Close Binary Systems | 25 Years of the Disk-Instability Model*, Mineshige S., Wheeler J.C., eds., Universal Academy Press, p. 147
16. Makita M., Miyawaki K., Matsuda T., 2000, *MNRAS*, 316, 906
17. Mathieu R.D., Adams F.C., Latham D.W., 1991, *AJ*, 101, 2184
18. Matsuda T., Inoue M., Sawada K., Shima E., Wakamatsu K., 1987, *MNRAS*, 229, 295
19. Matsuda T., Sekino N., Shima E., Sawada K., Spruit H., 1990, *A & A*, 235, 211
20. Matsuda T., Makita M., Bon H.M.J., 1999, In: *Disk Instabilities in Close Binary Systems | 25 Years of the Disk-Instability Model*, Mineshige S., Wheeler J.C., eds., Universal Academy Press, p. 129
21. Matsuda T., Makita M., Yukawa H., Bon H.M.J., 1999, In: *Numerical Astrophysics*, Miyama S.M., Tomisaka K., Hanawa T., eds., Kluwer, p. 207
22. Matsuda T., Makita M., Fujiwara H., Nagae T., Haraguchi K., Hayashi E., Bon H.M.J., 2000, *Ap&SS*, 274, 259
23. Menou K., 2000, *Science*, 288, 2022
24. Paczynski B., 1977, *ApJ*, 216, 822
25. Papalbizou J.C.B., Pingle J.E., 1977, *MNRAS*, 181, 441
26. Rozyczka M., Spruit H., 1989, In: *Theory of Accretion Disks*, Meyer F., Duschl W.J., Frank J., Meyer-Hofmeister E., eds., Kluwer, Dordrecht, p. 341
27. Rozyczka M., Spruit H.C., 1993, *ApJ*, 417, 677
28. Savonije G.J., Papalbizou J.C.B., Lin D.N.C., 1994, *MNRAS*, 268, 13
29. Sawada K., Matsuda T., Hachisu I., 1986, *MNRAS*, 219, 75
30. Sawada K., Matsuda T., Hachisu I., 1986, *MNRAS*, 221, 679
31. Sawada K., Matsuda T., Inoue M., Hachisu I., 1987, *MNRAS*, 224, 307
32. Shakura N.I., Sunyaev R.A., 1973, *A & A*, 24, 337
33. Soria R., Wu K., Hunstead R.W., 2000, *ApJ*, 539, 445
34. Spruit H., 1987, *A & A*, 184, 173
35. Spruit H.C., 1989, In: *Theory of Accretion discs*, Meyer F., Duschl W.J., Frank J., Meyer-Hofmeister E. (eds.), Kluwer, Dordrecht, p. 325
36. Spruit H.C., 2000, In: *The neutron star black hole connection*, C. Kouveliotou et al., eds., NATO ASI series
37. Spruit H., Matsuda T., Inoue M., Sawada K., 1987, *MNRAS*, 229, 517
38. Steeghs D., Harlaftis E.T., Homer K., 1997, *MNRAS*, 290, L28

39. Tout C A ., 2000, *New Astronomy Reviews*, 44, 37
40. Warner B ., 1995, *Cataclysmic variable stars*, Cambridge University Press
41. Watkins S J., Bhattal A S., Bon H M J., Francis N., Whitworth A P., *MNRAS*, 300, 1205
42. Watkins S J., Bhattal A S., Bon H M J., Francis N., Whitworth A P., *MNRAS*, 300, 1214
43. Whitehurst R., King A ., 1991, *MNRAS*, 249, 25
44. Whitworth A P., Bon H M J., Francis N., 1998, *A & G*, 39, 6.10
45. Yukawa H., Bon H M J., Matsuda T ., 1997, *MNRAS*, 292, 321